Rheol Acta
DOI 10.1007/s00397-006-0145-8

ORIGINAL CONTRIBUTION

# Rheological transitions in asymmetric colloidal star mixtures

**Christian Mayer · Emmanuel Stiakakis · Emanuela Zaccarelli · Christos N. Likos · Francesco Sciortino · Piero Tartaglia · Hartmut Löwen · Dimitris Vlassopoulos**

Received: 14 June 2006 / Accepted: 12 September 2006


**Abstract** We examine the rheological transition from an arrested to a fluid state for different mixtures of star polymers with varying functionality and size ratios. As a general trend, we find that addition of smaller star polymers in an arrested, concentrated solution of larger ones brings about melting of the large star glass. At the same time, the dependence of the amount of additives needed to melt the glass has a nontrivial dependence on the size ratio. Theoretical analysis, based on effective interactions and Mode Coupling Theory, reproduces the experimental results and helps identify two distinct types of glasses in the composite system.

This paper was presented at Annual European Rheology Conference (AERC) held in Hersonisos, Crete, Greece, April 27–29, 2006.

C. Mayer (✉) · C. N. Likos · H. Löwen
Institut für Theoretische Physik II: Soft Matter,
Heinrich-Heine-Universität Düsseldorf,
Universitätsstraße 1, 40225 Düsseldorf, Germany
e-mail: mayer@thphy.uni-duesseldorf.de

E. Stiakakis · D. Vlassopoulos
FO.R.T.H., Institute of Electronic Structure and Laser,
71110 Heraklion, Crete, Greece

E. Zaccarelli · F. Sciortino
Dipartimento di Fisica and CNR-INFM-SOFT,
Università di Roma La Sapienza, Piazzale Aldo Moro 2,
00185 Rome, Italy

P. Tartaglia
Dipartimento di Fisica and CNR-INFM-SMC,
Università di Roma La Sapienza, Piazzale Aldo Moro 2,
00185 Rome, Italy

D. Vlassopoulos
Department of Materials Science and Technology,
University of Crete, 71003 Heraklion, Crete, Greece

**Keywords** Rheology · Glasses · Star polymers · Mode coupling theory

## Introduction

Perhaps the most spectacular changes of the rheological state of a fluid are those encountered in the neighborhood of the *glass transition*, in which the many-body system runs into a state of *dynamical arrest*. Although dynamical arrest has no visible signature in the *structural* properties of the system, its dynamical response (viscosity, viscoelastic moduli, etc.) varies by orders of magnitude when external control parameters (temperature or concentration) are changed by tiny amounts. Accordingly, the understanding of the glass transition has been a topic of vivid interest for decades and it has experienced explosive growth in the realm of soft matter physics (Cates and Evans 2000; Vlassopoulos 2004; Larson 1999; Ediger 2000; Debenedetti and Stillinger 2001). Here, the ability to molecularly design various colloidal systems and chemically tune their architecture, composition, and physical characteristics opens up a wealth of novel scenarios and paths to various arrested states.

Recently a great deal of attention has been devoted to the study of the glassy states emerging in colloid–polymer (CP) mixtures, the former being hard, spherical colloids and the latter soft fractals. It has been found that the addition of a small amount of polymer brings about melting of the colloidal glass and, upon increase of the polymer concentration, a new *attractive* glass reemerges (Pham et al. 2002; Eckert and Bartsch 2002; Zaccarelli et al. 2002; Puertas et al. 2002), but this

phenomenon is restricted to a small range of polymer-to-colloid size ratios (Zaccarelli et al. 2004). Low-density dynamically arrested states, akin to a colloidal gel, arise when the colloids in the CP mixture have an additional long-range repulsion, the phenomenon being intricately connected to the formation of stable *clusters* in the system (Sciortino et al. 2004).

A different direction of investigation lies in replacing the hard glass-forming colloids with softer ones, such as star polymers (Grest et al. 1996; Vlassopoulos et al. 2001; Likos 2001). The ability to synthesize well-characterized and reasonably monodisperse stars, both in size and in arm number (functionality) has indeed promoted these systems into excellent models for studying the effects of *softness* in the glass formation. Similar to CP mixtures, it has been found that the addition of linear homopolymer melts the glass formed by the star polymers with functionality $f_1 = 122$ (Stiakakis et al. 2002a), but the range of size ratios for which this occurs is much broader than in CP mixtures. The possibilities to tailor the system's rheology grow even broader when large glass-forming stars of functionality $f_1 \gg 1$ are mixed with smaller ones with functionality $f_2 < f_1$. In this work, we present an extended and detailed account of recent experimental and theoretical findings on the glassy states of these composite systems (Zaccarelli et al. 2005). In Experiments, we show the results of rheological measurements, together with their compilation into a kinetic phase diagram, whereas in Theory, we present a detailed account of the theoretical description that reproduces and explains the experimental diagram. Finally, in Summary and conclusions, we summarize and draw our conclusions.

## Experiments

Different mixtures of small and large stars were measured. All large stars were synthesized using a dendrimer scaffold (Roovers et al. 1993) or a hydrosilylated 1,2-polybutadiene backbone (Roovers et al. 1989) and chlorosilane coupling chemistry to assemble living linear 1,4-polybutadiene arms and form colloidal stars with nominal functionality $f_1 = 128$ or 270. Small stars were synthesized with the dendrimer scaffold technique and yielded nominal $f_2 = 16$, 32 or 64 (Toporowski and Roovers 1986; Zhou et al. 1992). Table 1 lists the characteristics of the stars used in this study (extracted from Roovers et al. 1993, 1989; Toporowski and Roovers 1986; Zhou et al. 1992; Vlassopoulos 2004).

Several asymmetric binary mixtures were prepared. Most mixtures consisted of large stars of nominal $f_1 = 270$ (LS4, LS5, or LS6) at a high fixed concentration (about $1.4c^*$, $c^*$ being the overlapping concentration) in the glassy state (rheological solid); different small stars were added to these glasses, with varying functionality (18, 32, 64) and arm molecular weight (see Table 1), at different concentrations. Some mixtures consisted of a large star with nominal $f_1 = 128$, at the same volume fraction as the LS samples, in the glassy state; similarly, different small stars were added to this glass as well.

**Table 1** Summary of the physical properties of the polybutadiene stars used in the experiments

| Code | $f$ | $M_w$ ($10^6$ g/mol) | $R_h$ (nm) |
|---|---|---|---|
| 2518 | 19 | 0.541 | 20.0 |
| 3718 | 18 | 0.762 | 25.3 |
| 3210 | 31 | 0.301 | 11.5 |
| 3220 | 33 | 0.644 | 18.8 |
| 3237 | 35 | 1.33 | 27.2 |
| 3280 | 34 | 3.01 | 44.5 |
| 64015 | 56 | 0.0741 | 5.8 |
| 6405 | 57 | 0.258 | 12.3 |
| 6430 | 56 | 1.34 | 31.2 |
| 6460 | 61 | 2.89 | 49.6 |
| LS4 | 267 | 4.9 | 38.3 |
| LS5 | 269 | 7.9 | 50.7 |
| LS6 | 263 | 11.2 | 63.2 |
| 12880 | 122 | 8.8 | 64 |

The last four entries (separated from the rest by the horizontal line) denote the $f \gg 1$ systems that were kept at their vitrification concentration, whereas the preceding ones denote various stars of lower $f$ and smaller size that were used as additives.

Preparation of the mixtures involved forming the glassy state of the large star in toluene and adding the small star (under gentle and prolonged stirring, sometimes using excess solvent and subsequently evaporating to the desired concentration); the original glass was therefore *broken* and the mixture was then left still to *equilibrate* for at least 24 h. Special care was taken to reduce the risk of degradation by adding a small amount of antioxidant (Stiakakis et al. 2002b).

The state of a given sample was investigated with linear rheological measurements; they were carried out with a sensitive strain-controlled rheometer (Rheometric Scientific ARES-HR 100FRTN1). A cone-and-plate geometry (25 mm diameter, 0.04 rad cone angle) was used and the temperature was set at $20 \pm 0.1$ °C with a recirculating water/ethylene glycol mixture.

A homemade evaporation blocker system was used (with water as the *sealant* fluid in the area between the sample in the cone–plate fixture and an outer

ring; water content was controlled and renewed when needed), similar to that reported recently in the literature by Sato and Breedveld (2005). Once conditions for reproducible, time-independent, and linear measurements were established, small amplitude oscillatory shear measurements were performed in the frequency range 100–0.03 rad/s.

Typical results obtained with a mixture consisting of large stars with $f_1 = 122$ (coded 12880 in Table 1) and small stars with $f_2 = 32$ are depicted in Fig. 1. It is clear that the large star exhibits solid-like behavior, since $G' > G''$ and $G'$ is virtually frequency-independent. The particular frequency dependence of $G''$ is typical for a colloidal glass (Mason and Weitz 1995; Crassous et al. 2005; Raynaud et al. 1996). As we add the small star at constant functionality and molecular weight (sample 3210 in Table 1), the glass is weakened with increasing 3210 concentration, as judged by its rheological signal; more specifically, as $c_{3210}$ rises to 0.21% wt, the mixture's plateau modulus (high-frequency $G'$ limit) decreases substantially, i.e., by 42% with respect to the 12880 value (of 260 Pa). At the same time, the $G''$ remains virtually unchanged, suggesting that the key effect of the additive is the softening of the cage elasticity of the large stars. Eventually, at $c_{3210} =$ 0.5% wt, the cage apparently opens up, the glass melts, and the classic viscoelastic liquid response ($G' \sim \omega^2$, $G'' \sim \omega$, $G'' > G'$) is reached. This remarkable finding, particularly the change of viscoelastic moduli by orders of magnitude upon changing the concentration of the small star (here, basically doubling the concentration), suggests that linear rheological measurements serve as a very sensitive indicator of liquid-to-solid transitions. The same diagnostics has been applied also to determine, e.g., the rheology and dynamics of micellar solutions of block copolymers (Grandjean and Mourchid 2004). Note that the same behaviour is observed qualitatively when we keep the concentration of the added small star constant while changing its molecular weight (data are not shown here).

By using the rheological information obtained as outlined above, it is possible to construct a *kinetic state* diagram of concentration of the added small star against the ratio of hydrodynamic radii $\xi = R_h^{(32)}/R_h^{(128)}$, for constant $c_{12880} = 2.55\%$ wt. In this diagram, shown in Fig. 2, we map the rheological behavior of the star mixture as we change the additive. One can observe that by increasing the concentration of a given small star, the mixture is transformed from a solid (glass) to a viscoelastic liquid. On the other hand, at constant concentration of the small star, increasing its hydrodynamic radius yields a melting of the glass; eventually, for very large stars, there is an apparent tendency for a reentrant vitrification of the mixture. This upturn becomes more pronounced for different parameters, as has been shown by Zaccarelli et al. (2005).

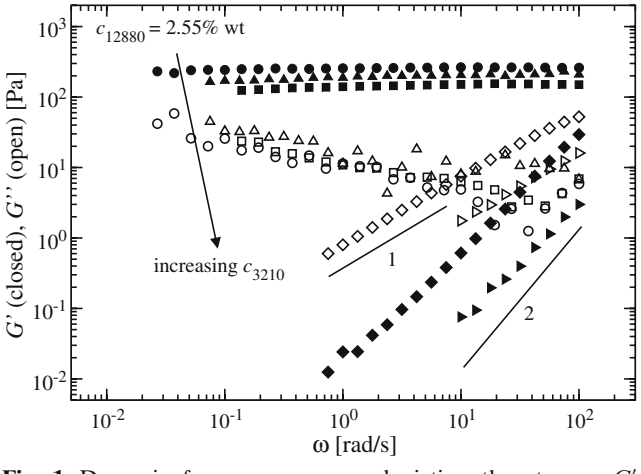


**Fig. 1** Dynamic frequency sweeps depicting the storage $G'$ (*closed symbols*) and loss $G''$ (*open symbols*) moduli as function of frequency for different mixtures consisting of a large star coded 12880 at $c_{12880} = 2.55\%$ wt and a small star coded 3210 at different concentrations: $c_{3210} = 0\%$ (*circles*), $c_{3210} = 0.066\%$ (*triangles*), $c_{3210} = 0.21\%$ (*squares*), $c_{3210} = 0.50\%$ (*diamonds*), $c_{3210} = 0.82\%$ (*triangles to the right*). Note that for *solid samples*, $G' > G''$ holds, whereas the opposite is true for fluid ones. *Solid lines* with slopes *1* and *2* represent the terminal scaling for $G''$ and $G'$, respectively

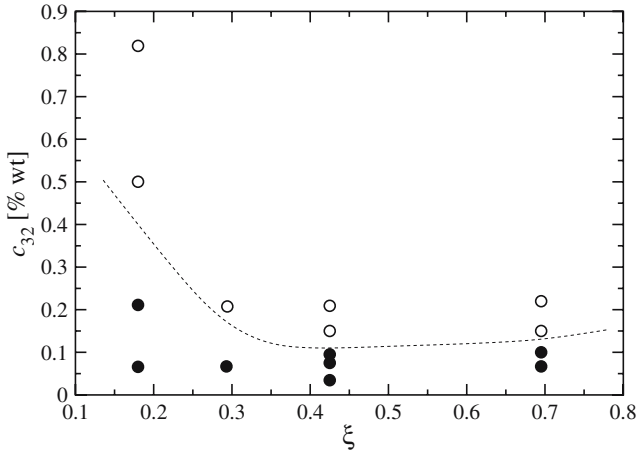


**Fig. 2** Experimental kinetic phase diagram of the binary star mixture consisting of a large star 12880 at $c_{12880} = 2.55\%$ wt in the glassy state and a small star with $f = 32$ arms at different molecular weights. *Open symbols* refer to a rheological liquid and *bold symbols* to a solid. The *dotted curve* is a guide to the eye

## Theory

### Structure of the system

We consider a binary mixture of $N_1$ large stars of functionality $f_1$ and $N_2$ smaller ones of functionality $f_2$ in a macroscopic volume $V$. The theoretical description of the binary star–polymer mixture is based on the knowledge of the three partial structure factors of the system, which describe the correlations between the centers of the stars. To calculate these data, we use the concept of effective interactions (Likos 2001) between the star cores. In this coarse-grained method, the monomer degrees of freedom are traced out and the star polymers are modeled as soft colloids, an approach pertinent to the problem at hand, as indeed the monomers continue to fluctuate even in the glassy state and only the stars as whole objects arrest. Thus, the positions of the star centers and the correlations between the same are the dynamical degrees of freedom of interest. They interact via an ultrasoft pair potential that depends on their relative separation.

The effective interaction between particles of species $i$ and $j$ reads as (von Ferber et al. 2000):

$$\beta V_{ij} = \Theta_{ij} \begin{cases} -\ln\left(\dfrac{r}{\sigma_{ij}}\right) + \dfrac{1}{1+\sigma_{ij}\kappa_{ij}} & \text{for } r \le \sigma_{ij}; \\ \dfrac{1}{1+\sigma_{ij}\kappa_{ij}} \left(\dfrac{\sigma_{ij}}{r}\right) \exp(\sigma_{ij}\kappa_{ij} - r\kappa_{ij}) & \text{else,} \end{cases} \tag{1}$$

where $\sigma_{ij} = (\sigma_i + \sigma_j)/2$, $2/\kappa_{ij} = \sigma_i/\sqrt{f_i} + \sigma_j/\sqrt{f_j}$, and

$$\Theta_{ij} = \frac{5}{36}\frac{1}{\sqrt{2}-1}\left[(f_i+f_j)^{3/2} - \left(f_i^{3/2} + f_j^{3/2}\right)\right].$$

Here, $\beta = (k_B T)^{-1}$ is the inverse temperature, with $k_B$ being the Boltzmann's constant and $\sigma_i$ is the corona diameter of species $i$ that turns out to coincide numerically with the corresponding hydrodynamic radius $R_h^{(i)}$ (Zaccarelli et al. 2005). Accordingly, we define the size ratio of the system $\xi$ as

$$\xi \equiv \frac{\sigma_2}{\sigma_1} < 1. \tag{2}$$

The origin of this interaction is entropic, therefore the potential scales linearly with temperature.

The structure of the system can be calculated by solving the two-component Ornstein–Zernike (OZ) equation with the Rogers–Young (RY) (Rogers and Young 1984) closure. In the two-component case, the OZ equation reads as (Hansen and MacDonald 2006):

$$\tilde{\mathsf{H}}(q) = \tilde{\mathsf{C}}(q) + \tilde{\mathsf{C}}(q)\mathsf{D}\tilde{\mathsf{H}}(q), \tag{3}$$

where $\tilde{\mathsf{H}}(q)$ and $\tilde{\mathsf{C}}(q)$ are symmetric $2 \times 2$ matrices with

$$\left[\tilde{\mathsf{H}}(q)\right]_{ij} = \tilde{h}_{ij}(q) \qquad \text{and} \qquad \left[\tilde{\mathsf{C}}(q)\right]_{ij} = \tilde{c}_{ij}(q). \tag{4}$$

$\mathsf{D}$ is a diagonal $2 \times 2$ matrix containing the number densities $\rho_i = N_i/V$ of the two species

$$[\mathsf{D}]_{ij} = \rho_i \delta_{ij}. \tag{5}$$

The total correlation functions $h_{ij}(r)$ $(i, j = 1, 2)$ are related to the radial distribution functions via $h_{ij}(r) = g_{ij}(r) - 1$, whereas the $c_{ij}(r)$ are the direct correlation functions of the system.

Due to the symmetry of the interactions, $h_{ij} = h_{ji}$ holds. Therefore, the OZ equation (Eq. 3) provides three equations for the six unknown functions $h_{ij}$ and $c_{ij}$. To compute these functions, we need additional three closure equations. For the kind of soft mixtures we investigate, the Rogers–Young closure turns out to be very accurate. In the multicomponent version, it reads as (Likos 2001):

$$g_{ij}(r) = \exp\left[-\beta V_{ij}(r)\right]\left[1 + \frac{\exp[\gamma_{ij}(r)\, f(r)] - 1}{f(r)}\right]. \tag{6}$$

Here $\gamma_{ij}(r) = h_{ij}(r) - c_{ij}(r)$ and $f(r) = 1 - \exp(-\alpha r)$ $(\alpha > 0)$. The value for the parameter $\alpha$ is determined by requiring the equality of the *fluctuation* and *virial* total compressibilities of the system (Rogers and Young 1984; Mayer et al. 2004). For $\alpha \to 0$, one obtains the Percus–Yevick closure, while for $\alpha \to \infty$, the hypernetted chain closure.

Another important quantity to characterize the structure of the system is the structure factor of the system, which is defined as $S_{ij}(q) = \delta_{ij} + \sqrt{\rho_i \rho_j}\tilde{h}_{ij}(q)$.

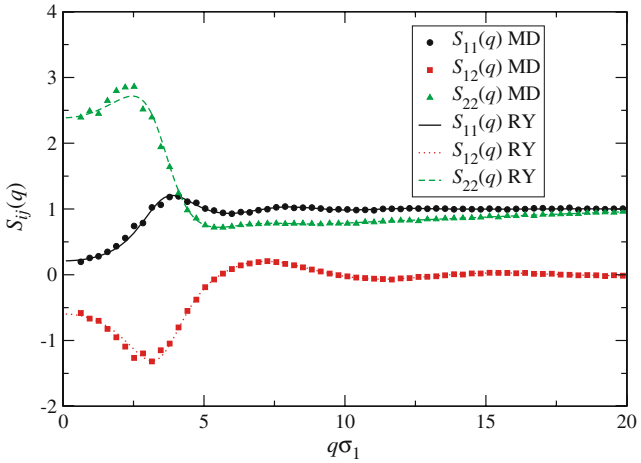


**Fig. 3** Partial structure factors of the binary mixture from molecular dynamics simulations (*MD*) and Rogers–Young theory (*RY*). Here the parameters are $f_1 = 270$, $f_2 = 32$, $\rho_1\sigma_1^3 = 0.1$, $\rho_2\sigma_1^3 = 10$, and $\xi = 0.1$

Figure 3 contains a comparison of structure factors of the system, as obtained from molecular dynamics simulations and from solving the OZ equation with the RY closure.[1] The RY approximation provides an excellent description of the structural properties of the mixture.

## Mode coupling theory

Having obtained the structural input, we now employ Mode Coupling Theory (MCT) to investigate the glass transitions. In general, MCT allows to study structural relaxations of supercooled liquids. Since we are only interested in the shape of the vitrification line in the phase diagram, we only calculate the long-time limit of the density correlators $\phi_{ij}(q,t)$, defined as

$$\phi_{ij}(q,t) = \left\langle \rho_i^*(q,0)\rho_j(q,t)\right\rangle / \left\langle \rho_i^*(q,0)\rho_j(q,0)\right\rangle, \tag{7}$$

with

$$\rho_i(q,t) = \sum_{l=1}^{N_i} \exp\left[i\mathbf{q}\cdot\mathbf{r}_l^{(i)}\right],$$

with $N_i$ being the number of particles of species $i$ and $\mathbf{r}_l^{(i)}$ the coordinates of the $l$-th particle of species $i$, and the asterisk denotes the complex conjugate. The nonergodicity parameters $f_{ij}(q)$ are then given by

$$f_{ij}(q) = \lim_{t\to\infty} \phi_{ij}(q,t). \tag{8}$$

MCT in a mixture can be applied in two different versions: one-component or binary. In the one-component case, it is assumed that the small stars in the system remain ergodic (mobile component); thus, the long-time dynamics of the mixture is determined entirely by the large ones. Accordingly, the prediction for the dynamics of the overall system is based only on the structure of the large stars, of course, taking into account its modification through the presence of the small ones by solving the full two-component OZ equations. However, only the structure factor of the large stars is used as input for the one-component MCT. In the limit $t\to\infty$, the one-component MCT equation reduces to

$$\frac{f_{11}(q)}{1-f_{11}(q)} = \frac{1}{2}\int \frac{\mathrm{d}^3k}{(2\pi)^3} V(\mathbf{q},\mathbf{k})\, f_{11}(k)\, f_{11}(|\mathbf{q}-\mathbf{k}|), \tag{9}$$

with

$$V(\mathbf{q},\mathbf{k}) = \frac{\rho_1}{q^4}\left[\mathbf{q}\cdot(\mathbf{q}-\mathbf{k})\tilde{c}_{11}(|\mathbf{q}-\mathbf{k}|) + \mathbf{q}\cdot\mathbf{k}\tilde{c}_{11}(k)\right] \times S_{11}(q)S_{11}(k)S_{11}(|\mathbf{q}-\mathbf{k}|), \tag{10}$$

where $c_{11}(q)$ is the Fourier transform of the direct correlation function. Equation 9 always admits the solution $f_{11}(q)=0$, which corresponds to an ergodic state where all correlations are lost in the $t\to\infty$-limit. However, when there are multiple solutions, MCT predicts that the one with the largest $f_{11}(q)$ is the real long-time limit (Götze 1991) of the density correlators.

In the two-component description, we include all the partial structure factors as described by Götze and Voigtmann (2003). Here, we consider a matrix $\mathsf{f}$ of the partial non-ergodicity parameters:

$$[\mathsf{f}(q)]_{ij} = f_{ij}(q).$$

The long-time limit is in this case given by

$$\mathsf{f}(q) = \bar{\mathsf{S}}(q) - \left\{\bar{\mathsf{S}}(q)^{-1} + \mathscr{F}[\mathsf{f}](q)\right\}^{-1}, \tag{11}$$

where the matrix $\bar{\mathsf{S}}(q)$ depends on the partial structure factors in the form

$$\left[\bar{\mathsf{S}}(q)\right]_{ij} = \sqrt{x_i x_j}S_{ij}(q), \tag{12}$$

where $x_i = N_i/(N_1+N_2)$ is the number concentration of species $i$. $\mathscr{F}[\mathsf{f}](q)$ is given by

$$\mathscr{F}_{ij}[\mathsf{f}](q) = \frac{1}{2q^2}\frac{\rho}{x_i x_j}\sum_{mnm'n'}\int \frac{\mathrm{d}^3k}{(2\pi)^3} V_{imm'}(\mathbf{q},\mathbf{k}) \times f_{mn}(k)\, f_{m'n'}(p) V_{jnn'}(\mathbf{q},\mathbf{k}), \tag{13}$$

with $\rho=\rho_1+\rho_2$. The vertices $V_{imm'}(\mathbf{q},\mathbf{k})$ are determined by the equilibrium structure of the system as

$$V_{imm'}(\mathbf{q},\mathbf{k}) = \frac{\mathbf{q}\cdot\mathbf{k}}{q}\tilde{c}_{im}(k)\delta_{im'} + \frac{\mathbf{q}\cdot(\mathbf{q}-\mathbf{k})}{q}\tilde{c}_{im'}(|\mathbf{q}-\mathbf{k}|)\delta_{im}.$$

The major difference between the two approaches is the treatment of the small component, which, in the two-component approach, is dealt with on equal footing as the large stars. Thakur and Bosse (1991a) show the size ratio dependence of the non-ergodicity parameter in binary hard sphere mixtures, where the ergodic to non-ergodic transition is consistent with our results (Fig. 4). The plot shows the development of the large and small star non-ergodicity parameters ( $f_{11}(q)$ and $f_{22}(q)$, respectively ) on increasing the size ratio. While $f_{11}(q)$ is virtually independent of $\xi$ (except for $\xi=0.3$ where the system is ergodic), $f_{22}(q)$ shows a dramatic change in the shape. For small $\xi$, $f_{22}(q)$ is nonzero only in a very small range of $q$. The length scale corresponding to the region is the size of the larger

[1] We simulated a system of 500 large and 5,000 small stars to calculate the structure factor. We let the simulation run for $10^6$ steps after equilibration.

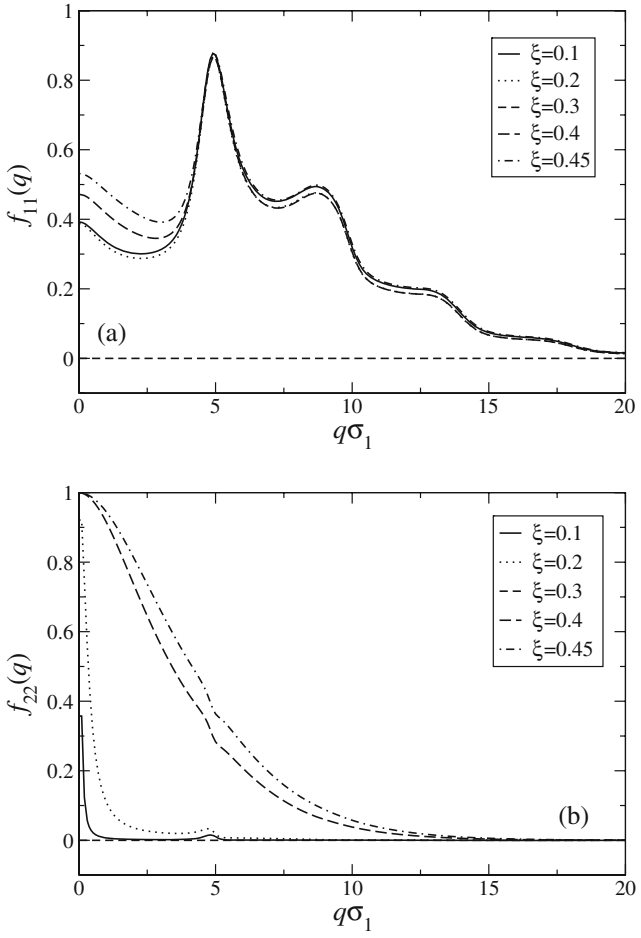


**Fig. 4** The nonergodicity factors $f_{11}(k)$ (**a**) and $f_{22}(k)$ (**b**) of the large and small components for $f_2 = 32$, $\rho_2\sigma_1^3 = 0.02$ for different $\xi$ values. Note that for $\xi = 0.3$, the system is ergodic

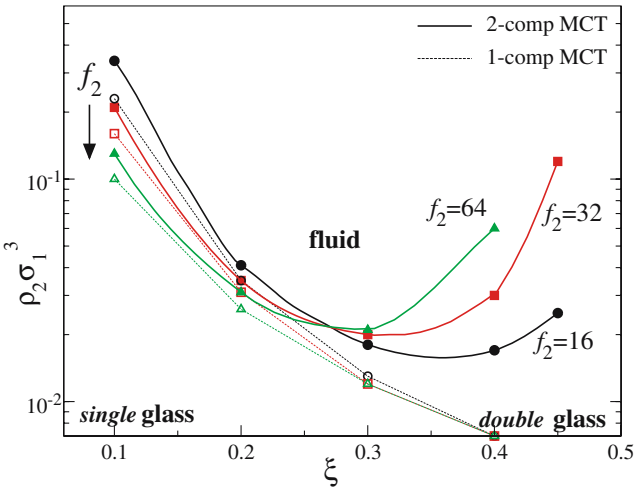


**Fig. 5** Kinetic phase diagram based on MCT calculations. The *points* trace the melting line separating the solid (*below*) from the fluid (*above*) behavior as predicted by one- and two-component MCT. The *lines* are guides for the eye. The large star functionality is $f_1 = 270$, the number density is kept constant at $\rho_1\sigma_1^3 = 0.345$. *Circles* $f_2 = 16$, *squares* $f_2 = 32$, *triangles* $f_2 = 64$

stars. This behavior can be interpreted in terms of a fluid small component (Thakur and Bosse 1991a,b). For large $\xi$, the system displays the behavior of a solid state.

## Phase diagram

We investigate how the dynamic properties of a solution of large star polymers can be influenced by small star additives. Figure 5 summarizes the result of the MCT calculations. We start from a glassy sample ($f_1 = 270$, $\rho_1\sigma_1^3 = 0.345$) and investigate the shape of the melting line as a function of the size ratio $\xi$ for different functionalities of small stars to show how the dynamics of the system depend on size and functionality of the additives. We find a U-shaped line separating the ergodic from the non-ergodic regions in the parameter space. A similar U-shape was found in the experimental data presented by Zaccarelli et al. (2005).

For small $\xi$, the melting of the glass can be interpreted in terms of a standard depletion mechanism where the small component remains mobile. This is corroborated by the fact that for small $\xi$, one- and two-component MCT yield the same trends and that the $f_{22}(q)$ in Fig. 4 show fluid-like behavior. The melting is driven by the fact that the depletion mechanism leads to a decrease of the repulsion between the large particles and, thus, to a softening of the cages. Within the effective one-component approximation, the depletion effect grows stronger with increasing $\xi$, as this leads to a concomitant increase of the depletion range and depth, i.e., to a more drastic effective weakening of the interstar repulsions. However, the essential question is whether the aforementioned one-component approximation indeed holds as $\xi$ increases.

For large $\xi$, the simple depletion scenario does not hold anymore. The smaller stars become now as large as the voids in the glassy matrix of the large ones and they can get trapped there, forming themselves a glass within the glass. The assumption of small star mobility breaks down. Therefore, the one-component MCT completely fails to describe the experimental results in the Experiments. Since the small stars become trapped in the cages formed by the large ones, they start to contribute to cage formation themselves. When $\xi$ grows, this trapping mechanism becomes more effective. This leads to a reversal of the slope of the vitrification line. Finally, the caging mechanism gets dominant, so that for $\xi > 0.45$ no melting is found within MCT. Therefore, we distinguish between two states under the melting line: a single glass when the small component remains mobile and a double glass when both species

become arrested. The same type of behavior is found in experiments of hard sphere mixtures with large size asymmetries (Imhof and Dhont 1995). However, in hard sphere mixtures, a melting of the large sphere glass upon adding the second component was not observed. This distinction is further supported by a quantitative analysis of the trends in the elastic moduli, presented below.

## Elastic modulus

The properties of the glass depend on the non-ergodicity parameters of the system. A quantity that readily allows comparisons with experiments is the elastic modulus $G'(\omega)$. The zero-frequency limit[2] $\omega \to 0$ of the modulus is given by Nägele and Bergenholtz (1998) and Bergenholtz and Fuchs (1999):

$$G' = \frac{k_B T}{60\pi^2} \int_0^\infty \mathrm{d}q\, q^4 \mathrm{Tr} \left[ \left( \rho \frac{\mathrm{d}\tilde{\mathbf{C}}(q)}{\mathrm{d}q} \bar{\mathbf{P}}(q, t \to \infty) \right)^2 \right], \quad (14)$$

where $\tilde{\mathbf{C}}(q)$ is the $2 \times 2$ matrix of the direct correlation functions defined in Eq. (4) and Tr stands for the trace of the resulting matrix. The matrix $\bar{\mathbf{P}}(q, t)$ is the dynamical generalization of Eq. (12) above:[3]

$$\left[\bar{\mathbf{P}}(q, t)\right]_{ij} = \sqrt{x_i x_j} S_{ij}(q, t) \quad (15)$$

and the long-time limit of the dynamic structure factors is given by

$$S_{ij}(q, t \to \infty) = S_{ij}(q)\, f_{ij}(q). \quad (16)$$

Clearly, in the ergodic state, $f_{ij}(q) = 0$, the elastic modulus $G'$ vanishes, whereas in non-ergodic states a finite result is obtained. The order of magnitude of the latter is set by $G' \sim k_B T/\sigma^3$, where $\sigma$ is the particle size, resulting into typical numbers $G' \sim 10^2$ Pa at room temperature.

In Fig. 6, we show the theoretical results for $G'$, demonstrating that, for $\xi \leq 0.3$, the elastic modulus has a (local) maximum at $\rho_2 = 0$, whereas for the larger size ratio, $\xi = 0.4$. It has a minimum there: the double glass displays a higher mechanical resistance to shear than the single one, whereas in the latter, the fluid-like second component does not contribute to $G'$. Its effect is to lower $G'$ through the softening of the cages

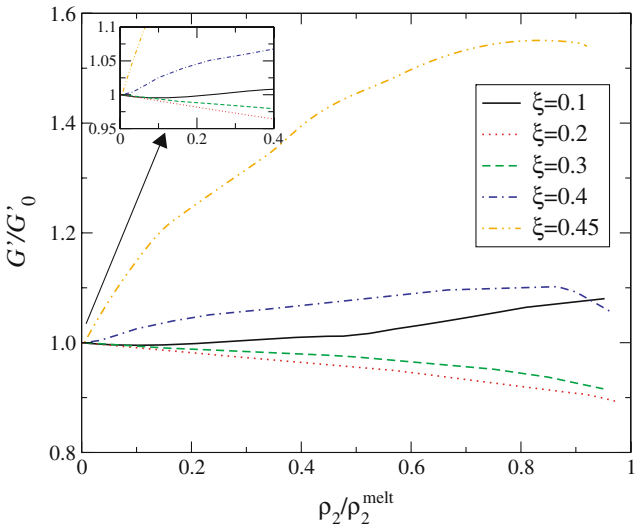


**Fig. 6** Plot of $G'/G'_0$, where $G'_0$ is the elastic modulus of the pure one-component system, as a function of depletion density, for different size ratios $\xi$. The *inset* is the magnification of the small $\xi$ region

formed by the large component.[4] These findings offer additional support to the single/double glass picture put forward above. Indeed, at the small $\xi$ regime, the small star polymers act as agents that tend to break the cages of the large stars without taking part in glass formation themselves. Accordingly, they lower the total elastic modulus. But as $\xi$ grows and the additives actively participate to cage formation themselves, they contribute in the elastic modulus in their own right, leading to an increase of its value up to a factor 1.6. Similar trends have also been seen in the experiments (Zaccarelli et al. 2005). At fixed $\rho_2$, the $\xi$ dependence $G'$ is non-monotonic, showing a decrease up to $\xi \approx 0.4$ and a growth thereafter (Zaccarelli et al. 2005).

## Summary and conclusions

We have presented experimental and theoretical results on the ways in which the rheology of soft colloidal systems can be influenced by the addition of chemically identical but physically distinct additives. Colloidal star polymers, which have been used in the present study, indeed provide a clean, versatile, and controllable

[2]The term zero-frequency (or $t \to \infty$) refers here to the ideal MCT result, according to which the glass (a nonequilibrium state) survives infinitely long.

[3]In this notation, $\bar{\mathbf{S}}(q) = \bar{\mathbf{P}}(q, t = 0)$, obtaining the equal-time, static structure factors.

[4]For $\xi = 0.1$, the maximum of $G'$ at $\rho_2 = 0$ in only local because as $\rho_2$ grows, a short-range attraction between the large stars develops leading to a temporary stabilization of the cages formed by the latter. This attraction is absent for higher $\xi$ values (see, e.g., Mayer et al. 2004).

system to this purpose. Contrary to colloid–polymer mixtures, the ability to melt the glass formed by the large component extends to large size ratios between the large stars and the smaller additives, a property whose physical origins can be traced back to the softness of the glass-forming component. Moreover, two distinct types of glasses have been identified, one in which the additives are ergodic at all concentrations and one in which they actively participate in cage formation, thus giving rise to a double glass. On the basis of the evidence at hand, we anticipate that there exists no sharp transition between the two types of glasses but rather a diffuse *crossover domain* because due to the softness of the pair interactions the movement of the small stars is not completely blocked, but becomes gradually slower. To answer this question, to address the issue of aging, and to draw a more complete *kinetic phase diagram* encompassing also the region of high additives concentration require more detailed theoretical and simulational work, as well as additional experimental measurements, employing rheology and dynamic scattering. Work along these lines is currently in progress.

**Acknowledgements** We are grateful to Jacques Roovers, Hermis Iatrou, and Nikos Hadjichristidis for providing the star polymers used in this work and for enlightening discussions. C.M. expresses his thanks to the Düsseldorf Entrepreneurs Foundation for financial support. This work has been supported by MIUR FIRB, MRTN-CT-2003-504712, by the EU within the Network of Excellence "Softcomp" and by the Deutsche Forschungsgemeinschaft within the Collaborative Research Centre SFB-TR6.

## References

Bergenholtz J, Fuchs M (1999) Nonergodicity transitions in colloidal suspensions with attractive interactions. Phys Rev E 59:5706–5715

Cates ME, Evans MR (eds) (2000) Soft and fragile matter: nonequilibrium dynamics, metastability and flow. Scottish Graduate Series, vol. 53. Institute of Physics, Bristol

Crassous JJ, Regisser R, Ballauff M, Willenbacher N (2005) Characterization of the viscoelastic behavior of complex fluids using the piezoelastic axial vibrator. J Rheol 49:851–863

Debenedetti PG, Stillinger FH (2001) Supercooled liquids and glass transition. Nature 410:259–267

Eckert T, Bartsch E (2002) Re-entrant glass transition in a colloid–polymer mixture with depletion attractions. Phys Rev Lett 89125,701

Ediger M (2000) Spatially heterogeneous dynamics in supercooled liquids. Annu Rev Phys Chem 51:99–128

Götze W (1991) Aspects of Structural Glass Transitions. In: Hansen J, Levesque D, Zinn-Justin J (eds) Liquids, freezing and glass transition. North-Holland, Amsterdam, p 287

Götze W, Voigtmann T (2003) Effect of composition changes on the structural relaxation of a binary mixture. Phys Rev E 67:021502

Grandjean J, Mourchid A (2004) Re-entrant glass transition and logarithmic decay in jammes micellar system. Rheology and dynamics investigation. Europohys Lett 65:712–718

Grest GS, Fetters LJ, Huang JS, Richter D (1996) Star polymers: experiment, theory, and simulation. Adv Chem Phys 94: 67–163

Hansen JP, MacDonald IR (2006) Theory of simple liquids, 3rd edn. Academic, London

Imhof A, Dhont JKG (1995) Experimental phase diagram of a binary colloidal hard-sphere mixture with a large size ratio. Phys Rev Lett 75:1662–1665

Larson RG (1999) The structure and rheology of complex fluids. Oxford, New York

Likos CN (2001) Effective interactions in soft condensed matter physics. Phys Rep 348:261–439

Mason TG, Weitz DA (1995) Linear visoelasticity of colloidal hard-sphere suspensions near the glass transition. Phys Rev Lett 75:2770–2773

Mayer C, Likos CN, Löwen H (2004) Equilibrium properties of highly-asymmetric star-polymer mixtures. Phys Rev E 70:041402

Nägele G, Bergenholtz J (1998) Linear viscoelasticity of colloidal mixtures. J Chem Phys 108:9893–9904

Pham KN, Puertas AM, Bergenholtz J, Egelhaaf SU, Moussaid A, Pusey PN, Schofield AB, Cates ME, Fuchs M, Poon WCK (2002) Multiple glassy states in a simple model system. Science 296:104–106

Puertas AM, Fuchs M, Cates ME (2002) Comparative simulation study of colloidal gels and glasses. Phys Rev Lett 88:098301

Raynaud L, Ernst B, Verge C, Mewis J (1996) Rheology of aqueous lattices with adsorbed stabilizer layers. J Colloid Interface Sci 181:11–19

Rogers FJ, Young DA (1984) New, thermodynamically consistent, integral-equation for simple fluids. Phys Rev A 30: 999–1007

Roovers J, Toporowski P, Martin J (1989) Synthesis and characterization of multiarm star polybutadienes. Macromolecules 22:1897–1903

Roovers J, Zhou LL, Toporowski PM, Vanderzwan M, Iatrou H, Hadjichristidis N (1993) Regular star polymers with 64 and 138 arms. Models for polymeric micelles. Macromolecules 26:4324–4331

Sato J, Breedveld V (2005) Evaporation blocker for cone-plate rheometry of volatile samples. Appl Rheol 15:390–397

Sciortino F, Mossa S, Zaccarelli E, Tartaglia P (2004) Equilibrium cluster phases and low-density arrested disordered states: the role of short-range attraction and long-range repulsion. Phys Rev Lett 93:055701

Stiakakis E, Vlassopoulos D, Likos CN, Roovers J, Meier G (2002a) Polymer-mediated melting in ultrasoft colloidal gels. Phys Rev Lett 89:208302

Stiakakis E, Vlassopoulos D, Loppinet B, Roovers J, Meier G (2002b) Kinetic arrest of crowded soft spheres in solvents of varying quality. Phys Rev E 66:051804

Thakur JS, Bosse J (1991a) Glass transition of two-component liquids. 1. The Debye–Waller factors. Phys Rev A 43:4378–4387

Thakur JS, Bosse J (1991b) Glass transition of two-component liquids. 2. The Lamb–Mössbauer factors. Phys Rev A 43: 4388–4395

Toporowski PM, Roovers J (1986) Synthesis and properties of 18-arm polybutadienes. J Polym Sci A Polym Chem 24:3009–3019

Vlassopoulos D (2004) Colloidal star polymers: models for studying dynamically arrested states in soft matter. J Polym Sci B Polym Phys 42:2931–2941

Vlassopoulos D, Fytas G, Pakula T, Roovers J (2001) Multiarm star polymers dynamics. J Phys Condens Matter 13:R855–R876

von Ferber C, Jusufi A, Watzlawek M, Likos CN, Löwen H (2000) Polydisperse star polymer solutions. Phys Rev E 62:6949–6956

Zaccarelli E, Foffi G, Dawson KA, Buldyrev SV, Sciortino F, Tartaglia P (2002) Confirmation of anomalous dynamical arrest in attractive colloids: a molecular dynamics study. Phys Rev E 66:041402

Zaccarelli E, Löwen H, Wessels PPF, Sciortino F, Tartaglia P, Likos CN (2004) Is there a reentrant glass in binary mixtures? Phys Rev Lett 92:225703

Zaccarelli E, Mayer C, Asteriadi A, Likos CN, Sciortino F, Roovers J, Iatrou H, Hadjichristidis N, Tartaglia P, Löwen H, Vlassopoulos D (2005) Tailoring the flow of soft glasses by soft additives. Phys Rev Lett 95:268301

Zhou LL, Hadjichristidis N, Toporowski PM, Roovers J (1992) Synthesis and properties of regular star polybutadienes with 32 arms. Rubber Chem Technol 65:303–314